Inorganic Chemistry

pubs.acs.org/IC

Communication

Mechanistic Investigation of the Synthesis of Dianionic In-Derived Coordination Polymers

Caleb J. Tatebe, Emily Fromel, Michael K. Bellas, Matthias Zeller, and Douglas T. Genna*

Cite This: *Inorg. Chem.* 2023, 62, 5881−5885

Read Online

ACCESS | Metrics & More | Article Recommendations | Supporting Information

ABSTRACT: The mechanism of formation of crystalline coordination polymers is as complex as the architectures themselves. In this Communication, we detail a three-tiered approach using density functional theory (DFT) analysis, synthesis, and *in situ* Raman spectroscopy to study the formation of coordination polymers. Specifically, the previously reported coordination polymers YCM-22 and YCM-51 containing the $[In(CO_2R)_2X_3]^{2-}$ (X = halogen) molecular building unit (MBU) were investigated. DFT revealed two potential pathways of formation, involving the initial formation of either $[InCl_4]^-$ or $[In(CO_2R)Cl_3]^-$. A molecular dimeric In species (**8a**) containing two $[In(CO_2R)Cl_4]^{2-}$ centers bridged by 2,5-thiophenedicarboxylic acid was isolated. When a suspension of **8a** was treated with a solution of 2,5-thiophenedicarboxylic acid, an isomer of the coordination polymer YCM-22 (denoted as YCM-22′) was formed. *In situ* Raman analysis of the formation of YCM-22 confirms that $[InCl_4]^-$ forms at the onset of the reaction and that the $[In(CO_2R)_2X_3]^{2-}$ MBU forms at its expense. The totality of the data presented support a mechanism of formation of one-dimensional In-derived coordination polymers and present a roadmap for future investigations into the formation of other crystalline coordination polymers.

Downloaded via OHIOLINK ACCESS ACCOUNT on July 2, 2023 at 14:34:11 (UTC).
See https://pubs.acs.org/sharingguidelines for options on how to legitimately share published articles.

The synthesis of crystalline coordination polymers including metal−organic frameworks (MOFs)[1] continues to be a highly active area of research due to their potential myriad applications as well as their synthetic and architectural complexities.[2−6] Studying the formation of these coordination polymers is quite challenging because there are several mechanistic regimes that occur either in solution, in the solid state, or at the solution−solid state interface. Liquid cell transmission electron microscopy,[7] atomic force microscopy,[8] X-ray scattering,[9] time-resolved X-ray diffraction,[10] UV resonance Raman,[11] and computational chemistry[12,13] have all been utilized to investigate this complex problem. Most studies have focused on nucleation (solution−solid state interface) and growth (solution−solid state interface and solid state) as opposed to coordination chemistry (solution). This focus on nucleation and crystal growth is understandable because nucleation is often considered rate-limiting,[14] and controlling the particle/crystal size has a direct impact on applications. Recent work by Brozek studied the solution effects of modulators on the nucleation of ZIF-8 and HKUST-1.[15] The role of modulators in general has been studied extensively and was recently reviewed by Forgan.[16] Modulators both affect the pH of the reaction through acid/base chemistry and can bind directly to the metal center, changing the ligand-displacement chemistry necessary for molecular building unit (MBU) formation.

To our knowledge, the first solution-phase studies of MOF formation were performed using ^1H and ^{27}Al NMR spectroscopy. This study demonstrated that hexaaquaaluminum monomers were the primary species in solution followed by formation of an Al(btc) (btc = 1,3,5-benzenetricarboxylate) complex in the synthesis of MIL-96, MIL-100, and MIL-101.[17] Using Raman and IR spectroscopies, Hartmann and Distaso have shown that the accumulation of aluminum carboxylate monomeric species in solution leads to nanoparticle-sized MIL-53(Al) and MIL-68(Al), while decreasing the amount of the aluminum carboxylate monomer yields micron-sized crystals.[18] Developing a detailed and nuanced understanding of the solution-phase chemistry of MOF formation is challenging. Herein we propose and demonstrate a multitiered and potentially broadly applicable approach using synthesis, density functional theory (DFT), and *in situ* Raman spectroscopy to study the formation of coordination polymers.

Previously, we reported the one-dimensional (1D) In-derived coordination polymers YCM-22[19] and YCM-51[20] (YCM = Youngstown Crystalline Material) synthesized from 2,5-thiophenedicarboxylic acid (H_2TDC) and terephthalic acid (H_2BDC), respectively. These coordination polymers are dianionic at In with $[In(CO_2R)_2X_3]^{2-}$ nodes where X = halogen, counterbalanced by $Me_2NH_2^+$ cations (Figure 1). The uncommon coordination environment (i.e., containing both halogen and carboxylate ligands) suggests that this In species could be a chemical intermediate in the formation of more common In-derived MBUs. As such, the formation of In centers of the type found in YCM-22 became an ideal test system for our multitiered approach and one that is relevant to the formation of more typical In-MBUs.

Received: January 13, 2023
Published: March 31, 2023

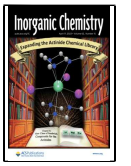

© 2023 American Chemical Society

https://doi.org/10.1021/acs.inorgchem.3c00148
Inorg. Chem. 2023, 62, 5881−5885

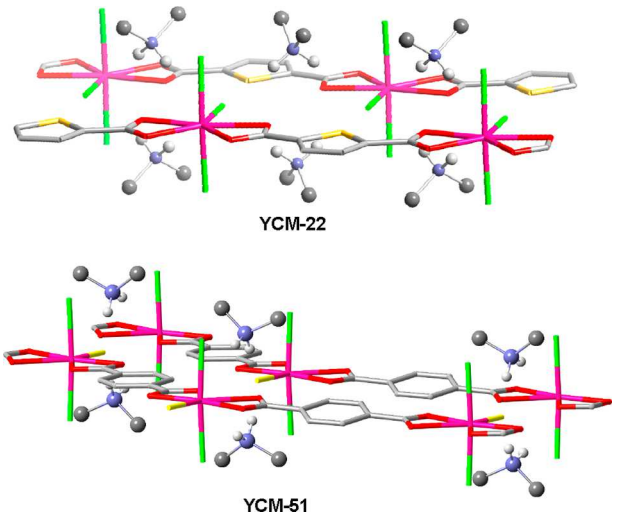

Figure 1. Structures of YCM-22 and YCM-51. H atoms attached to C atoms are omitted in structures for clarity. Color code: C, gray; O, red; In, magenta; Cl, green; S, yellow (YCM-22); F, yellow (YCM-51).

Previous work from our lab revealed that, upon dissolution, $InCl_3(H_2O)$ forms octahedral $InCl_3(DMF)_2(H_2O)$ (**1**; DMF = *N*,*N*-dimethylformamide).[21] Starting from **1**, we proposed that the MBU for YCM-22, $[In(CO_2R)_2Cl_3]^{2-}$ (**5**), could form by one of two possible pathways. The first proposed path (Figure 2, path a) commences with the displacement of water from In with a carboxylate ligand to form anionic intermediate **2**. While both DMF and water are displaceable ligands from In, calculations reveal that water is the more enthalpically labile ligand by 3.8 kcal/mol (relative to DMF) in this displacement [see the Supporting Information (SI): Additional Computational Analysis]. Dissociation of a DMF ligand from **2** allows the formation of the κ^2-carboxylate **3**. Subsequent loss of the second DMF ligand yields **4**, leaving an open coordination site for the second carboxylate ligand to associate and form the MBU **5**. Path b commences with the formation of octahedral solvated anionic $[InCl_4(DMF)_2]^-$ (**6**; Figure 2, path b). Intermediate **6** is proposed because YCM-22 is synthesized in the presence of HCl, providing an exogenous source of chloride in solution. Carboxylate displacement of a DMF ligand yields the dianionic complex **7**. Loss of the second DMF ligand allows for formation of the κ^2-carboxylate **8**. Complex **8** is transformed into the trianionic complex **9** featuring one κ^2-carboxylate and one κ^1-carboxylate. Loss of a chloride ligand then yields the product MBU **5**.

To better understand which pathway is more likely to be operable, solution-phase DFT calculations using the *QChem* software package were conducted using the ωB97X-D functional[22] and 6-31G* basis set for all non-In atoms, while the LANL2DZ-SV basis set[23] was used for In. DMF was modeled using a polarizable continuum implicit solvent model at 298.15 K. Compound **1** was used as the starting In source, Cl^- was modeled as free anionic chloride, and formate ion was used as the carboxylate ligand. Because the calculated intermediates are molecular in nature, the entropy of polymerization (and therefore ΔG) is not being considered; thus, our analysis is entirely enthalpic. The calculated enthalpies of the In species are summarized in Figure 3. For the transformation of **1** to **2** (Figure 3, path a), $\Delta H = -17.1$ kcal/mol represents an enthalpic minimum in path a. Formation of the κ^2-carboxylate **3** is uphill but still exothermic from the starting material. However, coordinatively unsaturated compound **4** represents the enthalpic maximum of the proposed reaction path, before undergoing a 30.3 kcal/mol (relative to **4**) downhill transformation to form the MBU **5**. Path b (Figure 3) begins with the formation of **6**, an enthalpically neutral transformation. Carboxylate displacement of DMF yielding **7** is the enthalpic minimum along this path. Formation of the κ^2-carboxylate **8** is uphill but still exothermic from **1**. Formation of **9** followed by formation of the MBU **5** are both exothermic. Because path a has an 11.1 kcal/mol enthalpic barrier relative to compound **1** and path b has no intermediates with higher relative enthalpy than the starting compound **1**, the computational analysis supports path b as being the most likely pathway.

To further explore the significance of path b, synthetic investigations were undertaken to isolate the proposed intermediates. Because all of the proposed intermediates are anionic (many are dianionic), we posited that the use of stabilizing cations would allow for isolation of the proposed intermediates. To this end, *N*,*N*-1,4-dipyridiniumbutane (DPB) was identified as an ideal counterion due to its dicationic nature and overall stability. Treatment of $InCl_3(H_2O)$ and H_2TDC with *N*,*N*-1,4-dipyridiniumbutane dichloride ($DPBCl_2$) in DMF/dioxane (3:2, v/v) at 70 °C (conditions analogous to the original YCM-22 synthesis)[19] led to the formation of a dimeric $[In(CO_2R)Cl_4]^{2-}$ species counterbalanced by two $[DPB]^{2+}$ cations (Figure 2), from here on referred to as dimer **8a** (Figure 4). We postulate that the reaction stops at **8a** instead of forming YCM-22 under these reaction conditions because the DPB cation forms a cagelike structure around the In-center. The cationic cage is then anchored in place by strong $\pi-\pi-\pi$ interactions between

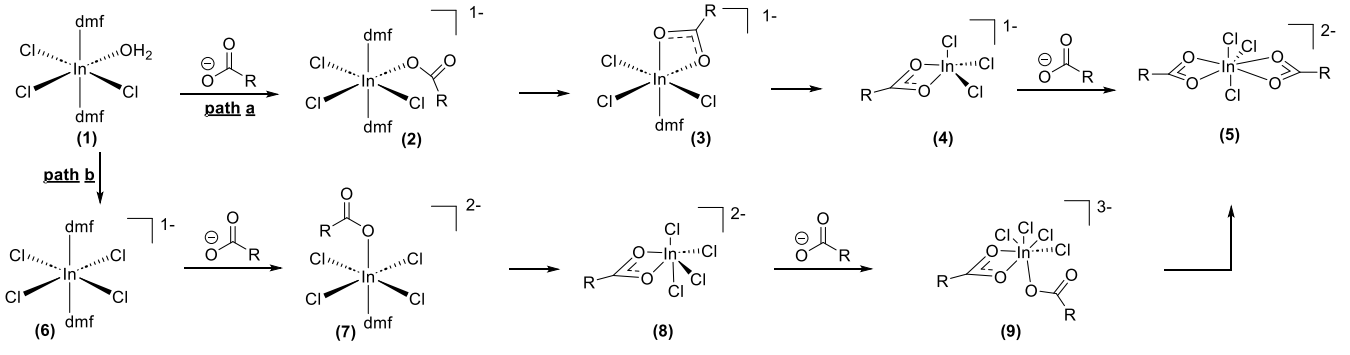

Figure 2. Proposed pathways for synthesis of the $[In(CO_2R)_2Cl_3]^{2-}$ MBU **5** from $InCl_3(dmf)_2(H_2O)$ (**1**).

https://doi.org/10.1021/acs.inorgchem.3c00148
Inorg. Chem. 2023, 62, 5881−5885

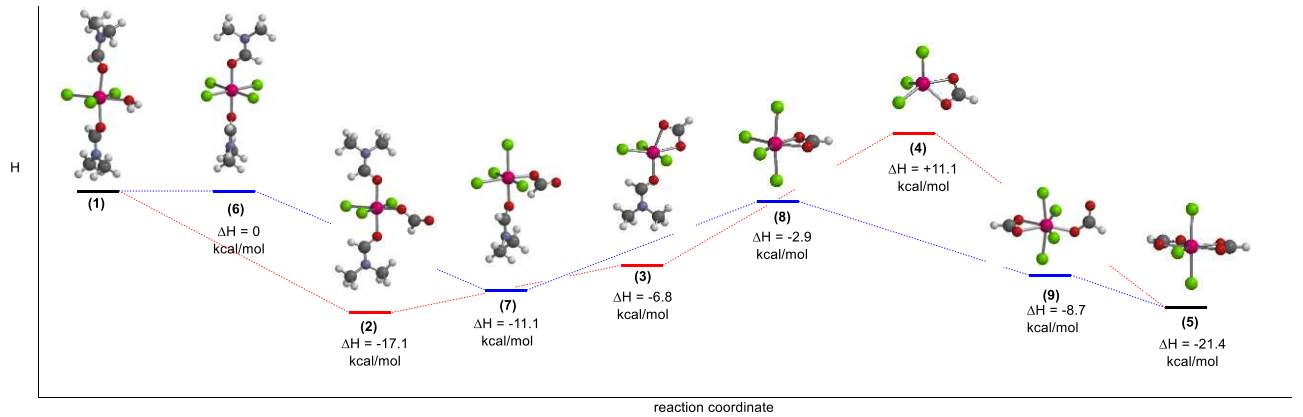

Figure 3. Path a (red) and path b (blue). All Δ*H* values are relative to the starting compound **1**. Color code: C, gray; H, white; O, red; N, blue; In, magenta; Cl, green.

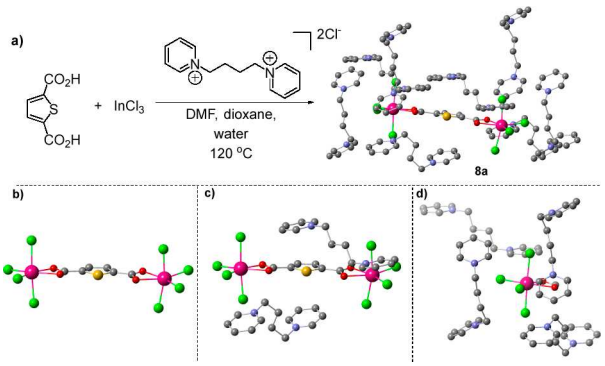

Figure 4. (a) Synthesis and structure of **8a**. (b) Structure of dimeric species without counterions. (c) $\pi-\pi-\pi$ stacking between thiophene and two pyridinium cations. (d) Cagelike enclosure surrounding In centers. H atoms are omitted in the structures for clarity. Color code: C, gray; H, white; O, red; N, blue; In, magenta; Cl, green; S, yellow.

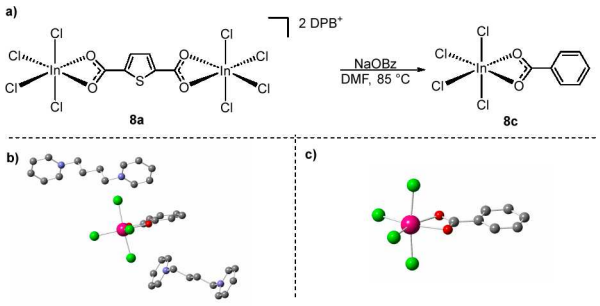

Figure 5. (a) Synthesis of **8c**. (b) Structure of **8c**. (c) Structure of **8c** without cations. H atoms are omitted in structures for clarity.

the cationic pyridiniums of two separate DPB ions and the electron-rich thiophene of the TDC linker (Figure 4c). An analogous structure of **8a**, referred to as **8b**, can be synthesized under similar conditions using H_2BDC instead of H_2TDC (Figures S12 and S13).

The reactivity of dimer **8a** was further explored to investigate whether it was an intermediate in the synthesis of YCM-22. Treatment of a suspension of dimer **8a** in DMF with 0.41 equiv of H_2TDC per In atom at 120 °C for 24 h yielded YCM-22′ (Figure S10). This structure gets the single prime notation because, unlike the original YCM-22 in which both carboxylates of the TDC linker are bound in a κ^2 fashion, in YCM-22′ each linker has one κ^2-carboxylate and one κ^1-carboxylate bound to In (Figure S10c). Additionally, the charge-balancing cation is DPB in YCM-22′, as opposed to $[Me_2NH_2]^+$ in YCM-22. Note that the MBU in YCM-22′ is analogous to intermediate **9** calculated in Figure 3. In contrast, treatment of dimer **8b** under analogous conditions using H_2BDC did not lead to polymerization but only yielded unreacted starting material.

Attempts to polymerize **8a** into mixed linker copolymers using H_2BDC and tetrafluoroterephthalic acid were unsuccessful and yielded only reisolated **8a**. Additionally, attempts to displace the In−Cl bonds with benzoic acid yielded no isolable product. However, treatment of **8a** with 3.3 equiv of sodium benzoate in DMF at 85 °C yielded monomeric $[InCl_4(benzoate)]^{2-}$ (**8c**; Figure 5). Monomer **8c** is still counterbalanced by the DPB cation; however, in the solid state, the $\pi-\pi-\pi$-stacking interaction found in dimer **8a** has been disrupted, and the DPB cations are participating in weak anion−π interactions with the chloride ligands bound to In. Note that, even with the addition of excess sodium benzoate *in situ* or to isolated **8c**, no displacement of In−Cl bonds was observed. Attempts to independently synthesize **8c** directly from $InCl_3(H_2O)$, $DPBCl_2$, and either sodium or silver benzoate yielded no isolable **8c** product.

In totality, the synthetic behavior of dimer **8a** implies that it is an intermediate in the synthesis of 1D coordination polymers such as YCM-22. It can polymerize into an isomer and potential precursor of YCM-22 (YCM-22′). Additionally, displacement of the TDC linker with benzoate implies that the species is capable of undergoing repair during self-assembly, which is critical for the formation of crystalline coordination polymers.

To further study the mechanistic pathway for the formation of **5**, we performed *in situ* Raman spectroscopy during the synthesis of YCM-22. Nearly instantaneous emergence of vibrations at 320 cm^{-1} indicates the rapid formation of an $[InCl_4]^-$ species.[21] This species grows in intensity for the first 5 h and then diminishes to trace levels over a period of 35 h (Figure 6). At 15 h, a vibration at 301 cm^{-1} grows in and persists for the duration of the experiment. Vibrations at 1458 and 1487 cm^{-1} are weakly present at the onset of the reaction but grow in intensity, reach their maximum at 31 h, and then persist. These vibrations are tentatively assigned to the MBU **5** based on comparative analysis with the solid-state Raman spectrum of YCM-22 (Figure S14). These data support that an $[InCl_4]^-$ species is present in solution and thus favor path b as

https://doi.org/10.1021/acs.inorgchem.3c00148
Inorg. Chem. 2023, 62, 5881−5885

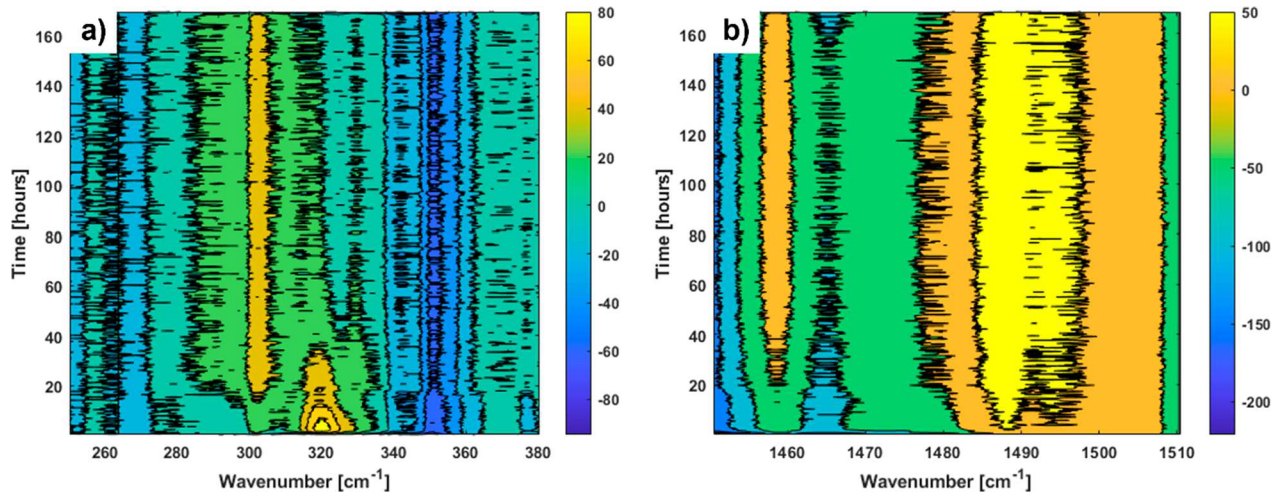

Figure 6. Dimensional contour plot of *in situ* Raman spectra of the synthesis of YCM-22: (a) 250−400 cm^{-1}; (b) 1450−1510 cm^{-1}. Note that the methods for solvent subtraction are detailed in the SI.

the likely mechanistic route. The rapidity in which the MBU **5** species forms is also notable when viewed in contrast to the length of reaction needed to precipitate YCM-22 (7 days). The relative slowness of precipitation may be due to slow chain growth in solution. This contention is consistent with our synthetic observation when dimer **8a** was treated with sodium benzoate, and the carboxylate ligand, rather than the chloride ligand, was displaced. While computationally this step is enthalpically downhill, the experimental difficulty in displacing the chloride implies a significant kinetic barrier to displacement.

In summary, DFT analysis of the proposed mechanistic pathways supports the formation of an $[InCl_4]^-$ intermediate before the formation of dimer **8a**. Two new polyanionic In dimeric species using dipyridinium salts (**8a** and **8b**) were synthesized. We hypothesize that these dipyridinium salts arrest typical coordination polymer growth by encapsulating the In center by participating in $\pi-\pi$ stacking with the linker of the dimer, allowing for the isolation of putative intermediates during self-assembly. Additionally, it was found that dimer **8a** could be treated with additional linker and be converted into YCM-22′, implying that dimers of the type **8a** are mechanistic intermediates in the synthesis of these types of coordination polymers. The presence of an $[InCl_4]^-$ intermediate was confirmed using *in situ* Raman spectroscopy. In totality, the synthetic, computational, and spectroscopic evidence support path b (Figure 2) as the most likely path for the formation of 1D coordination polymers containing $In(CO_2R)_2Cl_3]^2$ building units. We posit that the tools and strategies described should be applicable to the study of any coordination polymer synthesis. The roles of dimer **8a** and the MBU **5** as potential intermediates in the formation of $[In(CO_2R)_4]^-$ are being investigated using these tools and will be reported in due time.

■ ASSOCIATED CONTENT

Supporting Information

The Supporting Information is available free of charge at https://pubs.acs.org/doi/10.1021/acs.inorgchem.3c00148.

Experimental synthesis protocols, Raman spectroscopy, PXRD, and SCXRD (PDF)

Accession Codes

CCDC 2227116, 2227118−2227121, and 2234870 contain the supplementary crystallographic data for this paper. These data can be obtained free of charge via www.ccdc.cam.ac.uk/data_request/cif, or by emailing data_request@ccdc.cam.ac.uk, or by contacting The Cambridge Crystallographic Data Centre, 12 Union Road, Cambridge CB2 1EZ, UK; fax: +44 1223 336033.

■ AUTHOR INFORMATION

Corresponding Author

Douglas T. Genna − *Department of Chemistry, Youngstown State University, Youngstown, Ohio 44555, United States;* orcid.org/0000-0002-2407-8262; Email: dtgenna@ysu.edu

Authors

Caleb J. Tatebe − *Department of Chemistry, Youngstown State University, Youngstown, Ohio 44555, United States;* orcid.org/0000-0002-7817-388X

Emily Fromel − *Department of Chemistry, Youngstown State University, Youngstown, Ohio 44555, United States*

Michael K. Bellas − *Department of Chemistry, Youngstown State University, Youngstown, Ohio 44555, United States*

Matthias Zeller − *Department of Chemistry, Purdue University, West Lafayette, Indiana 47907, United States;* orcid.org/0000-0002-3305-852X

Complete contact information is available at: https://pubs.acs.org/10.1021/acs.inorgchem.3c00148

Notes

The authors declare no competing financial interest.

■ ACKNOWLEDGMENTS

We thank Professor Jeremy Feldblyum (SUNY Albany) for helpful discussions. This research was funded by National Science Foundation (NSF) Grant DMRRUI 1807462. The X-ray diffractometer was funded by NSF Grant DMR 1337296.

■ REFERENCES

(1) Seth, S.; Matzger, A. J. Metal−Organic Frameworks: Examples, Counterexamples, and an Actionable Definition. *Cryst. Growth Des.* **2017**, *17*, 4043−40481.

(2) Wei, Y.-S.; Zhang, M.; Zou, R.; Xu, Q. Metal-Organic Framework-Based Catalysts with Single Metal Sites. *Chem. Rev.* **2020**, *120*, 12089−12174.
(3) Wei, Y.-S.; Zhang, M.; Zou, R.; Xu, Q. Metal-Organic Framework-Based Catalysts with Single Metal Sites. *Chem. Rev.* **2020**, *120*, 12089−12174.
(4) Qian, Q.; Asinger, P. A.; Lee, M. J.; Han, G.; Mizrahi Rodriguez, K.; Lin, S.; Benedetti, F. M.; Wu, A. X.; Chi, W. S.; Smith, Z. P. MOF-Based Membranes for Gas Separations. *Chem. Rev.* **2020**, *120*, 8161−8266.
(5) Lu, X. F.; Fang, Y.; Luan, D.; Lou, X. W. D. Metal-Organic Frameworks Derived Functional Materials for Electrochemical Energy Storage and Conversion: A Mini Review. *Nano Lett.* **2021**, *21*, 1555−1565.
(6) Jones, C. W. Metal-Organic Frameworks and Covalent Organic Frameworks: Emerging Advances and Applications. *JACS Au* **2022**, *2*, 1504−1505.
(7) Patterson, J. P.; Abellan, P.; Denny, M. S., Jr.; Park, C.; Browning, N. D.; Cohen, S. M.; Evans, J. E.; Gianneschi, N. C. Observing the Growth of Metal-Organic Frameworks by *in* Situ Liquid Cell Transmission Electron Microscopy. *J. Am. Chem. Soc.* **2015**, *137*, 7322−7328.
(8) Cubillas, P.; Anderson, M. W.; Attfield, M. P. Crystal Growth Mechanisms and Morphological Control of the Prototypical Metal-Organic Framework MOF-5 Revealed by Atomic Force Microscopy. *Chemistry: A European Journal* **2012**, *18*, 15406−15415.
(9) Saha, S.; Springer, S.; Schweinefuss, M. E.; Pontoni, D.; Wiebcke, M.; Huber, K. Insight into Fast Nucleation and Growth of Zeolitic Imidazolate Framework-71 by In Situ Time-Resolved Light and X-ray Scattering Experiments. *Cryst. Growth Des.* **2016**, *16*, 2002−2010.
(10) Wu, Y.; Henke, S.; Kieslich, G.; Schwedler, I.; Yang, M.; Fraser, D. A. X.; O'Hare, D. Time-Resolved In Situ X-ray Diffraction Reveals Metal-Dependent Metal-Organic Framework Formation. *Angew. Chem., Int. Ed.* **2016**, *55*, 14081−14084. (b) Polyzoidis, A.; Etter, M.; Herrmann, M.; Loebbecke, S.; Dinnebier, R. E. Revealing the Initial Reaction Behavior in the Continuous Synthesis of Metal-Organic Frameworks Using Real-Time Synchrotron X-ray Analysis. *Inorg. Chem.* **2017**, *56*, 5489−5492.
(11) Petersen, T. D.; Balakrishnan, G.; Weeks, C. L. MOF crystal growth: UV resonance Raman investigation of metal-ligand binding in solution and accelerated crystal growth methods. *Dalton Transactions* **2015**, *44*, 12824−12831.
(12) Biswal, D.; Kusalik, P. G. Probing Molecular Mechanisms of Self-Assembly in Metal-Organic Frameworks. *ACS Nano* **2017**, *11*, 258−268.
(13) Cantu, D. C.; McGrail, B. P.; Glezakou, V.-A. Formation Mechanism of the Secondary Building Unit in a Chromium Terephthalate Metal-Organic Framework. *Chem. Mater.* **2014**, *26*, 6401−6409.
(14) (a) Stavitski, E.; Goesten, M.; Juan-Alcaniz, J.; Martinez-Joaristi, A.; Serra-Crespo, P.; Petukhov, A. V.; Gascon, J.; Kapteijn, F. Kinetic Control of a Metal-Organic Framework Crystallization Investigated by Time-Resolved In Situ X-ray Scattering. *Angew. Chem., Int. Ed.* **2011**, *50*, 9624−9628. (b) Millange, F.; El Osta, R.; Medina, M. E.; Walton, R. I. A time-resolved diffraction study of a window of stability in the synthesis of a copper carboxylate metal-organic framework. *CrystEngComm* **2011**, *13*, 103−108.
(15) Marshall, C. R.; Staudhammer, S. A.; Brozek, C. K. Size control over metal−organic framework porous nanocrystals. *Chemical Science* **2019**, *10*, 9396−9408.
(16) Forgan, R. S. Modulated self-assembly of metal−organic frameworks. *Chemical Science* **2020**, *11*, 4546−4562.
(17) Haouas, M.; Volkringer, C.; Loiseau, T.; Ferey, G.; Taulelle, F. In situ NMR, Ex situ XRD and SEM Study of the Hydrothermal Crystallization of Nanoporous Aluminum Trimesates MIL-96, MIL-100, and MIL-110. *Chem. Mater.* **2012**, *24*, 2462−2471.
(18) (a) Embrechts, H.; Kriesten, M.; Ermer, M.; Peukert, W.; Hartmann, M.; Distaso, M. Role of Prenucleation Building Units in Determining Metal-Organic Framework MIL-53(Al) Morphology. *Cryst. Growth Des.* **2020**, *20*, 3641−3649. (b) Embrechts, H.; Kriesten, M.; Ermer, M.; Peukert, W.; Hartmann, M.; Distaso, M. *In situ* Raman and FTIR spectroscopic study on the formation of the isomers MIL-68(Al) and MIL-53(Al). *RSC Adv.* **2020**, *10*, 7336−7348. (c) Embrechts, H.; Kriesten, M.; Hoffmann, K.; Peukert, W.; Hartmann, M.; Distaso, M. Distaso, Elucidation of the Formation Mechanism of Metal-Organic Frameworks via in-Situ Raman and FTIR Spectroscopy under Solvothermal Conditions. *J. Phys. Chem. C* **2018**, *122*, 12267−12278.
(19) Mihaly, J. J.; Zeller, M.; Genna, D. T. Ion Directed Synthesis of In-Derived 2,5-Thiophenedicarboxylate Metal Organic Frameworks: Tuning Dimensionality via Hydrogen Bond Donation. *Cryst. Growth Des.* **2016**, *16*, 1550−1558.
(20) Mihaly, J. J.; Tatebe, C. J.; Amirmokhtari, N.; DeSanto, M. J.; Zeller, M.; Genna, D. T. Halide-Directed Synthesis of an In-derived Metal-organic Framework with Two Unique Metal Centers and Isolation of its Potential Synthetic Precursor. *Cryst. Growth Des.* **2019**, *19*, 6053−6057.
(21) Tatebe, C. J.; Yusuf, S.; Bellas, M. K.; Zeller, M.; Arntsen, C.; Genna, D. T. On the Role of Dioxane in the Synthesis of In-Derived MOFs. *Cryst. Growth Des.* **2021**, *21*, 6840−6846.
(22) (a) Chai, J.-D.; Head-Gordon, M. Long-range corrected hybrid density functionals with damped atom−atom dispersion corrections. *Phys. Chem. Chem. Phys.* **2008**, *10*, 6615−6620. (b) Minenkov, Y.; Singstad, Å.; Occhipinti, G.; Jensen, V. R. The accuracy of DFT-optimized geometries of functional transition metal compounds: a validation study of catalysts for olefin metathesis and other reactions in the homogeneous phase. *Dalton Transactions* **2012**, *41*, 5526−5541.
(23) Chiodo, S.; Russo, N.; Sicilia, E. LANL2DZ basis sets recontracted in the framework of density functional theory. *J. Chem. Phys.* **2006**, *125*, 104107.

Recommended by ACS

Woven, Polycatenated, or Cage Structures: Effect of Modulation of Ligand Curvature in Heteroleptic Uranyl Ion Complexes
Sotaro Kusumoto, Pierre Thuéry, *et al.*
MAY 11, 2023
INORGANIC CHEMISTRY
READ

Structure and Magnetic Properties of Pseudo-1D Chromium Thiolate Coordination Polymers
Andrew Ritchhart, John S. Anderson, *et al.*
FEBRUARY 02, 2023
INORGANIC CHEMISTRY
READ

Incorporating Highly Anisotropic Four-Coordinate Co(II) Ions within One-Dimensional Coordination Chains
Tao Long, Yuan-Zhu Zhang, *et al.*
MARCH 13, 2023
CRYSTAL GROWTH & DESIGN
READ

Construction of High Quantum Yield Lanthanide Luminescent MOF Platform by In Situ Doping and Its Temperature Sensing Performance
Shiying Liu, Weisheng Liu, *et al.*
JUNE 12, 2023
INORGANIC CHEMISTRY
READ

Get More Suggestions >

https://doi.org/10.1021/acs.inorgchem.3c00148
Inorg. Chem. 2023, 62, 5881−5885